The Thesis committee for Terry Hurley Stevenson
Certifies that this is the approved version of the following thesis:

Design and Testing of a 3D Printed Propulsion System for Small Satellites

APPROVED BY

SUPERVISING COMMITTEE:

Wallace Fowler, Supervisor

E. Glenn Lightsey, Co-Supervisor

Design and Testing of a 3D Printed Propulsion System for Small Satellites

by

Terry Hurley Stevenson, B.S.As.E.

THESIS

Presented to the Faculty of the Graduate School of

The University of Texas at Austin

in Partial Fulfillment

of the Requirements

for the Degree of

MASTER OF SCIENCE IN ENGINEERING

THE UNIVERSITY OF TEXAS AT AUSTIN

May 2015

To Fred.

Acknowledgments

Dr. E. Glenn Lightsey, for being an excellent advisor and mentor for the past two years, and for trusting me to work on spaceflight missions as a student.

Dr. Wallace Fowler, for his insight and encouragement, and for leading the TSL through our transition.

Travis Imken, for letting me help with the INSPIRE thruster project, and for teaching me how to design a system that will actually work.

Sean Chait and the Prox-1 team, for giving us the opportunity to participate in this exciting mission.

Cody Colley, for his assistance designing, building, and testing the Prox-1 thruster, and for his limitless optimism.

Dr. Henri Kjellberg, for his constant support and brainstorming help, and for working to shape the outstanding lab culture of the TSL.

Sean Horton, for teaching me how to lay out a PCB and helping to design and program the Prox-1 electronics.

Parker Francis, for always being available for a mechanical engineering consult.

Design and Testing of a 3D Printed Propulsion System for Small Satellites

Terry Hurley Stevenson, M.S.E.
The University of Texas at Austin, 2015

Supervisor: Wallace Fowler
Co-Supervisor: E. Glenn Lightsey

A cold gas propulsion system for small spacecraft orbital maneuvers was developed by the University of Texas at Austin's Texas Spacecraft Laboratory. The thruster will allow the Prox-1 spacecraft, developed by the Georgia Institute of Technology, to conduct small scale maneuvers in Earth orbit. 3D printing was used to create a geometrically complex design at a low cost, and allowed the thruster to make efficient use of the available volume. The system was equipped with an onboard microcontroller that provides precise timing for firings, and can collect data from various sensors to send to the flight computer. The testing of this thruster focused on determining the level of thrust available and the specific impulse of the system. The thrust was found to be considerably higher during short pulses (2 milliseconds) than during long pulses (10 milliseconds), from 50 ± 16 mN to 35 ± 2.4 mN, respectively. The specific impulse was found to be 55.4 ± 17.7 seconds, which is sufficient to provide the Prox-1 thruster with a required velocity change of 15 m/s. A testing unit of the thruster was assembled and delivered in January of 2015, and the flight unit is scheduled for delivery in summer of 2015.

Table of Contents

List of Tables

List of Figures

Chapter 1

Introduction

Small satellites are an established part of modern space exploration, and in the past decade they have grown greatly in capability. One area of capability that small satellites are developing is propulsion systems. The development of miniature propulsion systems will enable small satellites to rendezvous with other space objects without relying on larger vehicles for transportation. It is also an important enabling technology for interplanetary small spacecraft, which will require propulsion systems for trajectory correction maneuvers and attitude control. In its Strategic Roadmap, NASA has identified micropropulsion as an area of high priority [1].

1.1 Contributions

The purpose of this thesis is to guide the reader through the design and testing process of a 3D printed cold gas thruster for a small satellite mission. The thruster has improved upon previous similar thrusters primarily in the area of instrumentation and control. The testing of this thruster focused on characterizing the uncertainty of the various parameters of the thruster (such as thrust and propulsive efficiency), to establish a range of possible values. This error characterization had been absent from previous cold gas thruster testing, and is necessary for more precise applications. The thruster is being developed for the Georgia Institute of

Technology's Prox-1 mission, and will enable the Prox-1 spacecraft to maneuver in orbit relative to another small satellite. This will allow testing of navigation and control algorithms developed for autonomous spacecraft rendezvous. The thruster test unit was delivered to Georgia Tech in the spring of 2015, and the flight unit will be assembled and delivered in the summer of 2015.

1.2 Thesis Organization

This thesis is divided into seven chapters. Chapter 2 explains the motivation for small satellites in general, and miniature cold gas thrusters specifically. Chapter 3 describes the design process of the thruster system, and the expected performance of the unit. Chapter 4 describes the apparatus used to test the system, and what parameters were measured. Chapter 5 discusses the data collected in the testing process and presents an analysis of the data. Chapter 6 outlines several recommendations for future thrusters based on lessons learned in this project. Finally, Chapter 7 concludes the thesis and summarizes the work completed.

Chapter 2

Motivation

In the past decade, small spacecraft have assumed an increasingly important role in both commercial and government spaceflight. Companies such as Planet-Labs are taking advantage of the low cost and short development times of small satellites to reduce the cost of space-based services [2]. In the case of Planet-Labs, the company has deployed a constellation of small satellites, each one approximately the size of a loaf of bread. These satellites carry cameras to provide quickly-updating imagery of a large part of Earth's surface.

Government agencies are also turning to small satellites to reduce budgetary pressures and shorten mission development times. NASA's Ames Research Center launched a small satellites called GeneSat in 2006 to study the effects of spaceflight on microorganisms. GeneSat helped lead the way for NASA's small spacecraft program by proving that such missions have scientific value [3]. The low cost of small satellites also puts space exploration within reach of smaller nations. Estonia recently launched its first satellite, EstCube, a cubic satellite measuring only 10 cm on each side [4]. Despite its small size, EstCube is capable of determining its orientation, taking pictures and sending those pictures to its control center in Estonia.

Many university groups have also formed to develop missions on small

satellite platforms. The low cost of small satellites has put them within reach of university research groups operating on limited budgets. The fast development cycle also lends itself well to a university environment, in which the primary workforce of students has a relatively high turnover rate.

2.1 Texas Spacecraft Laboratory

One such university group is the Texas Spacecraft Laboratory. The Texas Spacecraft Laboratory (TSL) is a research laboratory in the University of Texas at Austin's Department of Aerospace Engineering and Engineering Mechanics. The TSL's principal investigator is Dr E Glenn Lightsey, and consists of approximately six graduate students and ten undergraduate students. The lab has delivered spaceflight hardware for five missions since its inception, with two more missions currently under development.

Most recently, the TSL designed, built, tested, and delivered the Radiometer Atmospheric CubeSat Experiment (RACE) to NASA's Jet Propulsion Laboratory (JPL). RACE's flight software, structure, and attitude control system were designed by the TSL, and JPL provided RACE's scientific instrument: a radiometer designed to study water vapor in Earth's upper atmosphere. RACE's entire life cycle lasted only 11 months from initial funding to delivery, showing the ability of small satellites to reduce mission turnaround. The TSL also designed and built a satellite ground station to carry out command and control of RACE. Unfortunately, RACE was destroyed in the Antares Orb-3 launch mishap in October 2014.

The TSL has two more missions under development. Bevo 2 is a satellite

built as part of NASA Johnson Space Center's LONESTAR program (Low Earth Orbiting Navigation Experiment for Spacecraft Testing Autonomous Rendezvous and Docking). Bevo 2 will be deployed from the International Space Station with another small satellite, built by Texas A&M, and will use a small cold gas thruster to maneuver relative to the Texas A&M satellite. Bevo 2 is expected to launch in late 2015.

The second mission in development is ARMADILLO (Atmosphere Related Measurements and Detection of Submillimeter Objects). ARMADILLO is being developed under the United States Air Force's University Nanosatellite Program (UNP). ARMADILLO will perform GPS occultation experiments using a UT Austin-developed GPS receiver, and provide in-situ dust detection [5]. ARMADILLO is currently planned for launch in early 2016.

The TSL has also contributed to JPL's INSPIRE (Interplanetary NanoSpacecraft Pathfinder In Relevant Environment) mission. The TSL designed, built, and tested a four-nozzle cold gas thruster to provide attitude control for the INSPIRE spacecraft. The thruster was designed using heritage from the Bevo 2 thruster, but was more extensively characterized. This experience in small satellite cold gas technology led the Prox-1 team to select the TSL to design and assemble the thruster for that mission.

2.2 Cold Gas Propulsion Systems

A cold gas propulsion system is a propulsion system that derives all of its energy from a gas held under pressure[6]. Cold gas systems do not perform any

combustion or substantial heating of the propellant; the thruster simply releases the propellant directly through a nozzle. Cold gas propulsion systems are typically simple relative to combustion systems. They also require fewer parts, so more of the volume of the system can be devoted to propellant storage. Finally, they are safer to handle and test than combustion systems, because of the inert nature of the gas. However, cold gas systems are also less energetic than combustion systems, since they can only release the energy stored by the pressure of the propellant. While attractive from a safety standpoint, this lower energy reduces the amount of momentum that the system can impart to a spacecraft.

Cold gas systems can use a wide variety of different propellants, but inert compounds are typically chosen for safety reasons. The propellant can be stored as a high pressure gas, such as carbon dioxide or nitrogen, or as a saturated liquid, such as freon. Storing the propellant as a saturated liquid typically allows higher densities at a given pressure, increasing the propellant's energy capacity within a fixed volume, but also restricts the propellant choice. The operating temperatures of a spacecraft are determined by its mission, so a substance must be chosen that has a saturation pressure across the temperature range that is not so low that it produces too little thrust, and not so high that the tank walls must unreasonably strong to withstand it.

On large spacecraft, combustion systems are typically chosen for the larger maneuvers that they allow, but cold gas thrusters are attractive options for small satellites for both attitude control and small translational maneuvers. Many small satellites are built by university groups, which may lack the facilities to handle more complex and dangerous propellants and propulsion systems. For example,

R-236fa, the propellant used by the Texas Spacecraft Laboratory for the Bevo 2 and INSPIRE thrusters, is an inert and nontoxic compound. The simplicity of cold gas systems also reduces development time and the cost per unit, both of which are factors driving the development of small satellites.

Cold gas thrusters have been previously used on small spacecraft. The Microelectromechanical System PICOSAT Inspector (MEPSI) was a 1.4 kg satellite designed by The Aerospace Corporation to inspect larger spacecraft, such as crewed vehicles or space stations[7]. MEPSI employed a small cold gas thruster filled with Xenon gas to maneuver relative to the object being inspected. The MEPSI prototype was deployed from STS-116, and demonstrated the possibility of using cold gas propulsion on a small satellite. The use of Xenon as a propellant limited the total ΔV capability of the unit to 0.4 m/s, but the system demonstrated thrust within the range expected.

2.3 3D Printing

Additive manufacturing, also called 3D printing, is a manufacturing process in which material is added layer by layer to a part to form a specific shape. This is in contrast to removal methods, in which a large stock piece is machined down to a specific shape. 3D printing is a large and varied industry with many different methods of printing and many different materials. 3D printers range from small units printing simple plastics marketed to consumers, to large, expensive machines capable of printing metals such as aluminum or stainless steel. Methods of printing range from heating and extruding plastic from a moving head to using a laser to

melt and fuse microscopic metal particles.

Many industries use 3D printing only to produce prototypes, and then use more traditional manufacturing methods for final components. However, 3D printing technologies have advanced to the point that 3D printed parts have a high enough quality to be used in final units. A 3D printer was sent to the International Space Station to produce parts and tools that would otherwise have to be sent on the next cargo mission [8]. This greatly reduces the time the astronauts must wait for new parts, which improves the efficiency of routine maintenance.

The advantages of 3D printing make it an attractive option for manufacturing small satellite components. The low cost and highly efficient use of volume are beneficial to small satellite missions that often have small budgets and restrictive volumes. In particular, propulsion systems are highly volume limited, so every bit of available volume is valuable. 3D printing allows the tanks to assume more versatile shapes that maximize the tank volume within the thruster. More tank volume allows more propellant to be carried, which allows the thruster to operate for longer periods before depleting its propellant.

The versatility of 3D printing allows geometries that would be prohibitively expensive and time consuming to produce through traditional machining. Specifically, complex internal features like curved pipes and irregular tanks can be printed directly into the plastic, producing a monolithic piece and greatly reducing the risk of leaks from seals and joints. Without the benefits of additive manufacturing, such parts would need to be made of many different pieces and sealed together. Each of these joints represents a potential leak, especially for a system that will undergo

vibrations, such as may be experienced by a spacecraft during launch.

3D printing offers other benefits to spacecraft component development. Unlike traditional machining, the cost of additive manufacturing does not increase with the complexity of the part, only the total size. Highly complex parts can thus be redesigned and printed quickly, allowing a rapid iterative design process. For example, the exact nozzle location can be easily moved from one design to the next to accommodate a change in the spacecraft's center of mass.

2.4 Prox-1 Mission

The Prox-1 satellite is being developed by the Georgia Institute of Technology's Space Systems Design Laboratory as part of the Air Force University NanoSatellite Program. UNP is a program run by the Air Force Research Laboratory that provides funding and launch opportunities to university small satellite programs [9]. The primary goal of UNP is educational: providing students with experience in spacecraft design, integration and operation. UNP also supports the development of university satellite programs, which in turns supports the development of new spacecraft technologies.

The primary mission of Prox-1 is to demonstrate autonomous relative navigation with a second satellite [10]. At launch, Prox-1 will carry a smaller satellite, measuring only 10x10x30 cm, inside a deployment pod. This satellite, called LightSail-B, is being developed by The Planetary Society to demonstrate solar sail deployment [11]. A computer aided design (CAD) model of Prox-1 is shown in Figure 2.1.

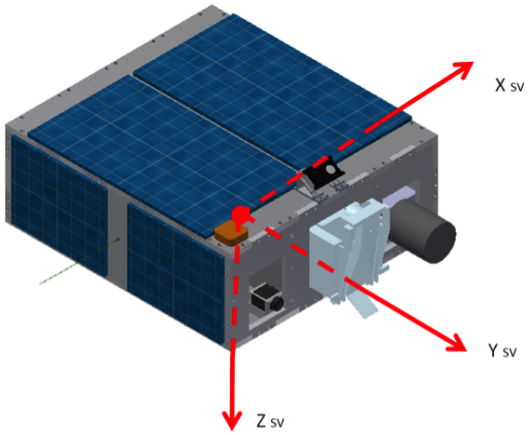

Figure 2.1: 3D model of the Prox-1 spacecraft, showing the principal axes, as well as the LightSail-B deployment pod (light blue).

Once the initial mission checkout phase is complete, and all of Prox-1's system are known to be functional, Prox-1 will open the deployer pod and release LightSail-B. Prox-1 will then use its onboard thermal imaging system to acquire LightSail-B, and compute the relative trajectories of the two spacecraft. No radio link between Prox-1 and LightSail-B will be used for this mission; the navigation will be based entirely on Prox-1's GPS unit and imaging system.

After Prox-1 acquires a relative navigation solution for LightSail-B, it will maneuver into an orbit that leads LightSail-B by 100 meters, and maintain that position for several orbits. It will then perform a circumnavigation of LightSail-B, moving around the smaller satellite into a 100 meter trailing position, and then back to a leading position. Once the relative stationkeeping and circumnavigation phases are complete, Prox-1 will use its imaging systems to observe LightSail-B's solar sail deployment.

In order to fulfill this mission, Prox-1 will require a thruster for translational maneuvers. This will enable it to carry out the small orbit changes required during the relative navigation phase. The Prox-1 team initially considered a combustion system, but eventually decided to procure a cold gas thruster from the TSL. This thruster is only needed for translational maneuvers (as opposed to rotational maneuvers), so only a single nozzle will be required.

Chapter 3

Thruster Design

This chapter describes the design process for the Prox-1 thruster. First, the general concept of operations of a cold gas thruster are discussed. Then the design requirements and a general overview are presented. Next, the design of the thruster's structure, tanks, and nozzle are examined, focusing on the design of the printed plastic structure as well as the metal interfaces. Then the component selection and the control system design are presented. Finally, the predicted performance calculations are discussed, using one-dimensional fluid flow equations.

3.1 Concept of Operations

The thruster will have two separate propellant tanks. The larger tank is called the "main tank". This tank holds the bulk of the propellant as a saturated liquid-vapor mixture. Storing the propellant as a saturated mixture allows a higher density of propellant than a pressurized gas, which allows a greater mass of propellant for the same tank volume. The second, smaller tank is called the "plenum". The plenum holds the propellant as a vapor only. The plenum acts as a buffer for the propellant, allowing it to expand from a liquid in a controlled way before being expelled through the nozzle. This arrangement is illustrated in Figure 3.1.

When the Prox-1 spacecraft is launched, the plenum will initially be evacu-

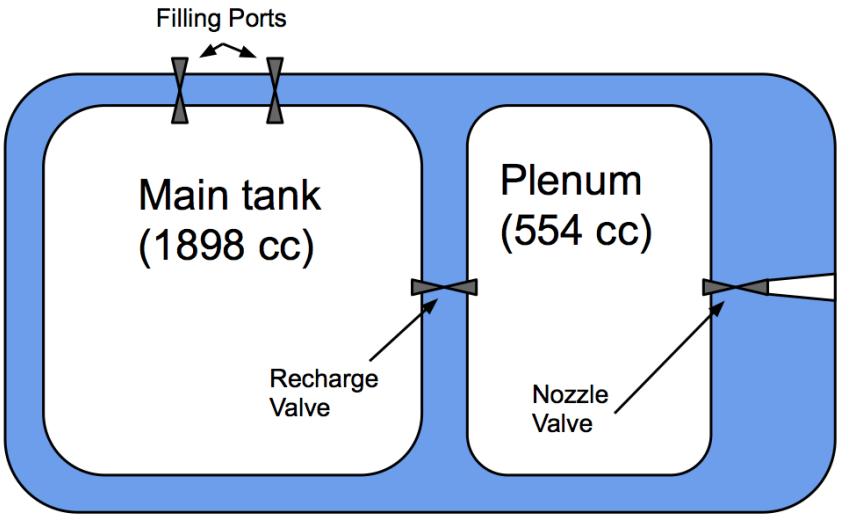

Figure 3.1: Conceptual diagram of the Prox-1 thruster, showing the valves and tanks. Note that this does not show the actual geometry of the thruster. The specifics of the volume allocation are discussed in Section 3.4.1.

ated. Before any maneuvers can be executed, the plenum will be filled with vapor from the main tank through the recharge valve, as shown in Figure 3.1. The propellant is then expelled from the plenum through the nozzle. As the thruster fires, the plenum pressure will decrease, and it will periodically be refilled from the main tank.

3.2 Design Requirements

The Prox-1 team levied a variety of requirements on the thruster design to ensure that it would be able to fulfill the mission. The principal requirements were a velocity change capability (also called ΔV), a minimum thrust level, and various electronic and software requirements. As the thruster design evolved, it

was constantly checked against these requirements to ensure that they were met.

3.2.1 Velocity Change

The most important design requirement of the thruster was that it be capable of providing a velocity change (ΔV) of 15 m/s for a spacecraft with a total spacecraft wet mass of 65 kg. The ΔV capability of a spacecraft can be found with the following equation:

$$\Delta V = g I_{sp} ln(\frac{m_O}{m_f}) \tag{3.1}$$

In Equation 3.1, g is the acceleration due to gravity (9.81 m/s^2), I_{sp} is the specific impulse of the propulsion system in seconds (55.4 seconds), m_0 is the initial mass of the spacecraft (65 kg including propellant), and m_f is the final mass of the spacecraft (initial mass minus propellant mass expelled). This equation is known as the Tsiolkovsky rocket equation [12]. The rocket equation is derived from Newton's Laws of Motion for an object that is expelling its own mass. This equation assumes that the exhaust velocity is constant, which requires the temperature and pressure of the propellant to be constant. This is not the case, but for a series of small maneuvers it is a reasonable approximation.

From Equation 3.1, given a ΔV, the required propellant can be calculated. The Prox-1 spacecraft will have a maximum of 59 kg of mass that is not part of the propulsion system (6 kg were allocated to the thruster and its propellant). The ΔV capability also depends on the structural, or "dry" mass of the thruster itself, which varied throughout the design process as the structure geometry changed. Ultimately,

the required propellant mass for this design was determined to be 1838 grams.

3.2.2 Thrust

The Prox-1 thruster was initially required to provide a minimum of 50 millinewtons of thrust for at least 10 seconds in a single burn at a 50% duty cycle. The thrust level requirement was met by sizing the nozzle appropriately, which is discussed in detail in section 3.8. The duration requirement was met by sizing the plenum to maintain the needed pressure throughout a 10 second burn.

Initially, the thruster was believed to require duty-cycling to sustain thrust for this long. In this mode of operation, the nozzle valve is repeatedly actuated to produce of series of short pulses of thrust to reduce the average mass flow rate out of the thruster. The Prox-1 thruster was intended to use a 50% duty cycle, in which the nozzle valve would be open for a short period, then closed for an equal period. Previous thrusters designed by the TSL required this mode. The Prox-1 thruster was ultimately designed to allow continuous operation, which not only effectively doubles the thrust produced, but also greatly reduces the power consumption of the valves.

3.2.3 Electronics

Another design requirement was that the thruster be capable of actuating with precise onboard timing. Previous thrusters have required every low level command to be issued by the spacecraft flight computer. This reduces the complexity of the thruster electronics, but increases the demand on the flight computer to issue rapid, precisely timed instructions. For example, the INSPIRE thruster is capable

of producing pulses as short as 2 milliseconds. This requires the flight computer to send "valve open" and "valve close" commands precisely 2 milliseconds apart. Given the other demands on the flight computer, and the typically low processor speeds of such devices, this can present a problem. Offloading this timing function to a dedicated microcontroller improves the precision of the thruster timing and reduces load on the flight computer. The Prox-1 thruster was designed to have such a microcontroller on the thruster electronics board, to provide precise timing and sensor data interpretation.

The thruster was also required to be fully instrumented. In order for Prox-1 to determine how and when to fire the thruster, the flight computer must have knowledge of the state of the propellant inside both the main tank and the plenum. The plenum propellant will be entirely vapor, so the pressure and temperature of the tank must be known. The main tank will contain a saturated liquid-vapor mixture until the very end of the mission, when the propellant is nearly depleted. In theory, if either the pressure or temperature of a saturated mixture is known, the other can be determined. However, due to concerns about sensor reliability in orbit, both a pressure and temperature sensor are included in the main tank.

3.2.4 Other Requirements

The thruster was also required to have a maximum total wet (fully fueled) mass of 6 kg. Given the previous requirement for 1838 grams of propellant, this allowed a maximum of 4162 grams of dry mass. This dry mass includes the printed structure, metal manifolds, fittings, fasteners, electronics, and wiring. The final dry mass of the Engineering Design Unit (EDU) thruster was 3584 grams. Fully

fuelled, the thruster was 578 grams under the mass budget. This additional mass will be redistributed to increase the mass margin of the other subsystems.

The thruster was given a limited volume within the Prox-1 spacecraft, measuring 20 cm x 20 cm x 18 cm. The thruster structure, propellant tanks, and electronics board were all required to fit within this envelope. The only part allowed to protrude was the nozzle, which had a maximum protrusion of 16 mm. Ultimately, not all of this volume was needed, and to save mass, the thruster was designed to a small envelope of 20 cm x 16 cm x 18 cm

The thruster was required to have a structural factor of safety of 2.5 on all expected pressures. This large factor of safety was required due to the relatively untested nature of 3D printed pressure vessels. Various other requirements were levied pertaining to physical and software interfaces, schedule, and budget. These played a role in the design process, but will not be discussed in detail here.

3.3 Design Overview

A CAD model of the Prox-1 thruster is shown in Figure 3.2. The bulk of the thruster is a single piece of 3D printed material, shown in Figure 3.2 in blue (the printed material is a light blue color once dried). The printed structure is hollow, and contains the two tanks, the propellant pipes, and baffling to reduce slosh of the propellant. The protruding feature on the front face of the thruster is the nozzle, surrounded by protective supports. The gray pieces shown are metal components that are used to provide an interface to the plastic for the sensors, valves, and filling ports. The green board on the front of the thruster is the electronics board.

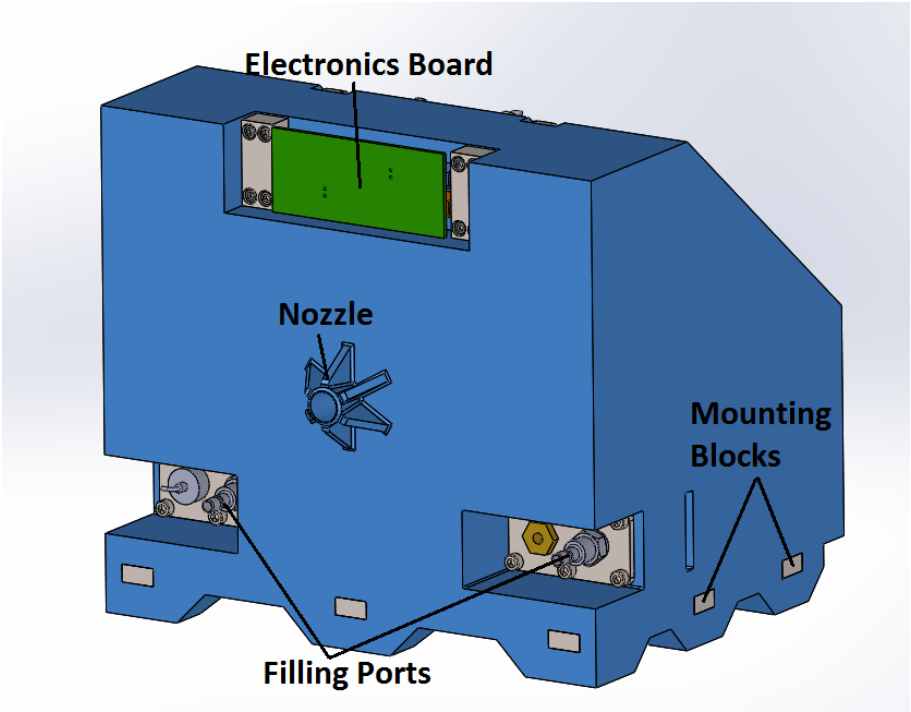

Figure 3.2: Outer view of the Prox-1 thruster, showing four of the manifolds, the filling ports, the mounting blocks, the electronics board, and the nozzle.

This printed circuit board holds the thruster's microcontroller, as well as the electronic switches that control power to the valves, and the signal conditioning for the thruster's sensors. The valves are located immediately behind the circuit board, and their leads are soldered directly to the board. The thruster is connected to the Prox-1 spacecraft via nine bolts. In Figure 3.2, five of the mounting blocks are visible at the bottom of the image. The mounting bolts pass through holes in the printed structure and thread into the mounting blocks to hold the thruster securely in place.

3.4 Structural Design

The thruster was designed to incorporate as many features as possible into the printed material. Printing the piping, nozzle and tanks into the same continuous piece of material reduces the risk of leaks. The design of the tanks, which comprise the bulk of the thruster's volume, are discussed first. The metal interfaces, necessary for sensors, fill ports and valves are discussed next. Finally, the nozzle design is described.

3.4.1 Printed Structure

The main tank must be large enough to accommodate the required mass of propellant. The propellant will be held in the main tank as a saturated liquid. If a saturated liquid is heated within a enclosed volume, the fraction of the volume occupied by liquid increases. The liquid itself has a lower density at higher temperatures, and as the liquid expands, the vapor is compressed and some of it condenses into liquid. As the mixture is heated, this process continues until the entire volume is occupied by liquid. At this point, if the liquid is heated further, the pressure increases rapidly. Compressibility information is not available for R-236fa, but liquids are generally modeled as incompressible due to the extreme pressures required for even small compressions. The thruster cannot be practically designed to withstand these pressures, so the main tank is sized to accommodate the full load of propellant at the maximum operating temperature while maintaining enough volume to allow some vapor to exist.

The Prox-1 spacecraft specifies 50°C as the maximum temperature. The liquid density of R-236fa at 50°C is 1270 kg/m^3 [13], so to accommodate 1838

grams of propellant, the main tank must be at least 1447 cubic centimeters. The main tank was actually sized to 1898 cm^3, to both provide margin to increase the safety of the thruster and also allow the Prox-1 team to increase the propellant mass to a maximum of 2.41 kg without requiring a redesign.

The main tank incorporated several protruding structures inside the main tank, called baffles. These structures are printed directly into the interior walls of the thruster, and will reduce the movement of the liquid propellant within the tank. Propellant slosh, as this movement is known, can cause problems for attitude control systems, since it represents non-rigid mass, the momentum of which is not directly controllable. Such structures are not needed in the plenum, since no liquid will be present.

The plenum was sized by the requirement that the thruster produce at least 95% of nominal thrust for at least 10 seconds without recharging the plenum. This requires a plenum of at least 454 cm^3. The EDU plenum was sized to 554 cm^3. Figure 3.3 shows a cutaway view of the thruster, showing the plenum and main tank. The total tank volume is 2452 cm^3, out of 5760 cm^3 in the reduced thruster envelope. The remainder of the volume was used for manifolds, piping, attachment points, and cutouts to reduce mass.

The tanks were designed to withstand the saturation pressure of the propellant at the maximum operating temperature, with a structural safety factor of 2.5. This requires that the thruster withstand at least 1.46 MPa of internal pressure. The walls were sized using finite element analysis in Solidworks using the mechnical properties of the Accura Bluestone material to ensure that they met the pressure

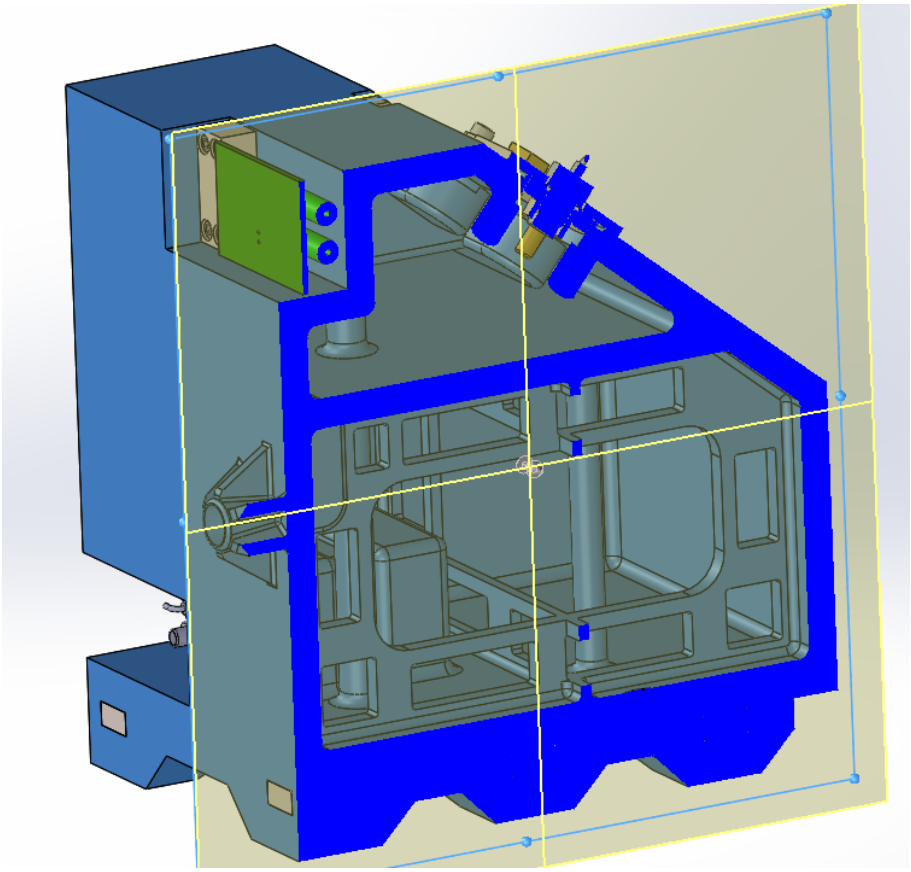

Figure 3.3: Cutaway view of the Prox-1 EDU thruster, showing the plenum (upper), and main tank (lower). Note the baffling structures inside the main tank.

requirement. The minimum wall thickness throughout the design is 8 mm.

3.4.2 Manifolds

The thruster was designed to take advantage of the versatility and low cost of the 3D printing process as much as possible, but some metal components were still required. The 3D printed material cannot be threaded reliably, so any component that pierces either tank must be threaded into a metal manifold, which is then sealed to the thruster with a o-ring face seal. This requires a compressive force, so fasteners must compress the manifold against a back plate. An example of this arrangement is shown in Figure 3.4, which shows a cutaway view of the manifold used to hold the main tank thermal probe and one of the filling ports. In this case, two components, a thermal probe and a filling port, are mounted on a single manifold (lower metal part). The manifold is pressed to the plastic by the tension in the six fasteners (three shown), which are threaded into the backplate. Each sensor enters the tank through a hole in the plastic structure. Each hole is surrounded by a printed groove that holds an O-ring. When the manifold is tightened, the O-ring deforms and fills the groove to prevent any leaks.

This complex arrangement has proven very reliable in preventing leaks, but also consumes a large amount of volume that could otherwise be used for propellant storage. This can be mitigated to a certain extent by using a single manifold for multiple sensors, as shown in Figure 3.4, but the manifold still intrudes on the tank volume substantially.

There are 5 manifolds total on the thruster, all of them made from 316 stainless steel. Two of them are in the main tank, and each one holds a filling port

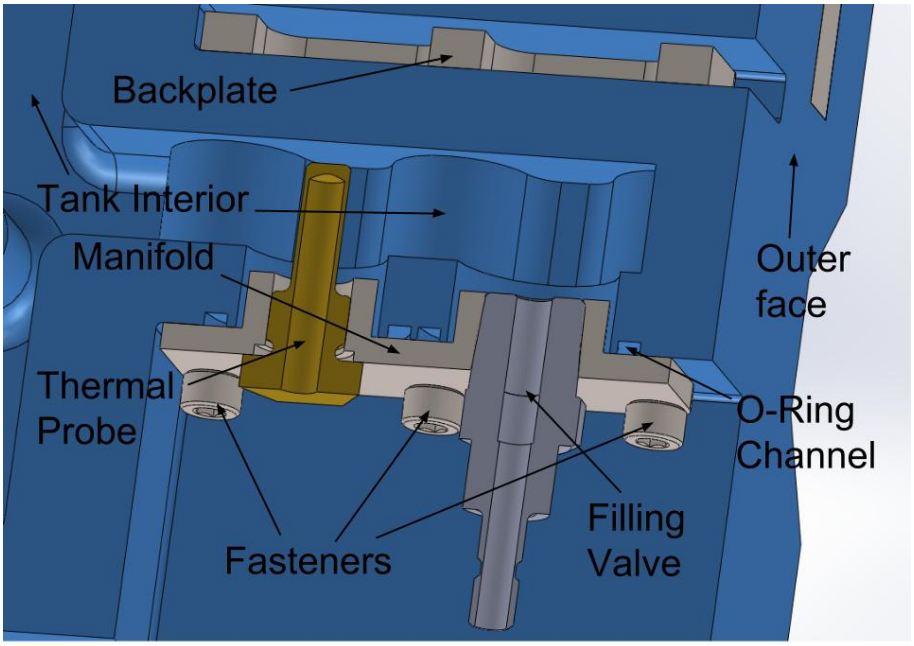

Figure 3.4: Cutaway view of a manifold seal (gray) with sensors (dark gray and bronze) against the main tank (blue). Note the large volume required for the manifold and supporting components.

and a sensor, either a pressure sensor or a thermal sensor. Two more connect to the plenum and are attached to the valves, and the final one holds the sensors for the plenum. Together, these manifolds, backplates and fasteners have a mass of 275 grams, and require an additional 150 grams of supporting material in the 3D printed structure. All of the manifold fasteners are attached with locking elements, either locking helical inserts or locknuts, to prevent loosening from vibrations.

3.4.3 Nozzle Design

The Prox-1 thruster, like many spacecraft propulsion systems, has a converging-diverging nozzle. This shape accelerates a high pressure gas past the speed of sound. Plots of gas properties and a nozzle profile are shown in Figure 3.5.

The nozzle accelerates the flow to the speed of sound at the throat of the nozzle (the location of least cross-sectional area), since a subsonic flow accelerates when the cross section is reduced [14]. The flow transitions to supersonic and continues to accelerate through the diverging section, since a supersonic flow accelerates when the cross section is *increased*. As the gas moves through the nozzle, its pressure and temperature decrease as it expands into the near-vacuum conditions outside the nozzle.

The nozzle of the thruster was printed as part of the thruster structure. In order to preserve internal volume for the propellant tanks, the nozzle protrudes from the structure by 16 millimeters, a limit defined by the Prox-1 team. As a protruding part, the nozzle is at risk of damage from being struck. To reduce this risk, six supporting features were added to the outside of the nozzle. These features serve to both reinforce the nozzle and to prevent other objects from striking it directly.

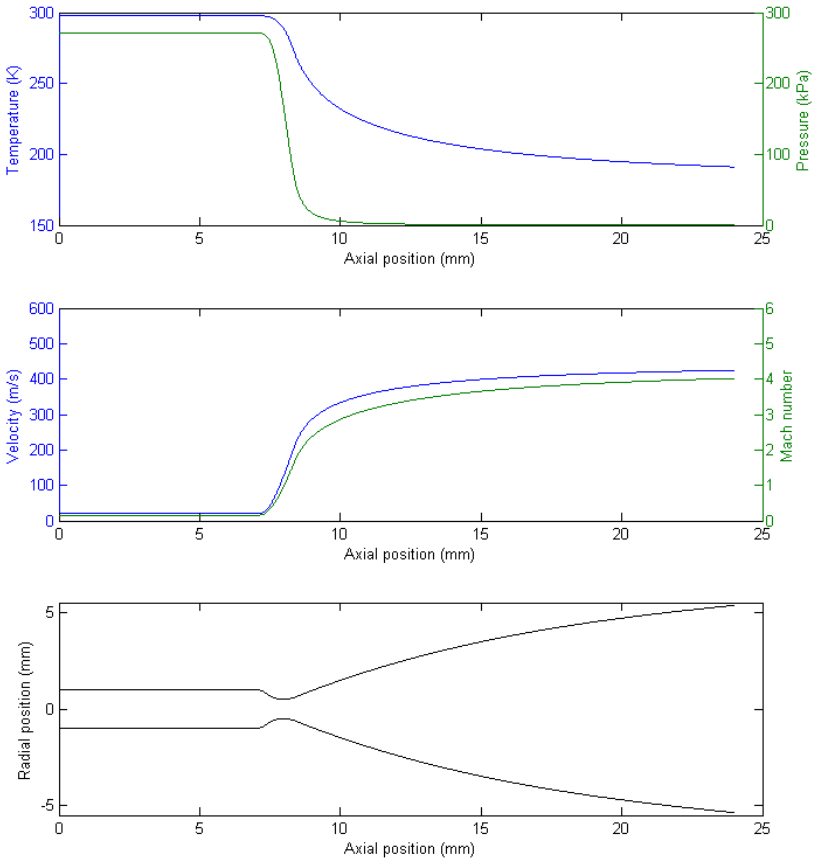

Figure 3.5: Properties of the flow through the Prox-1 nozzle, showing gas properties (top), velocity and Mach number (center) and nozzle profile (bottom). The throat occurs at 8 millimeters, note that this is the point at which the Mach number is 1.

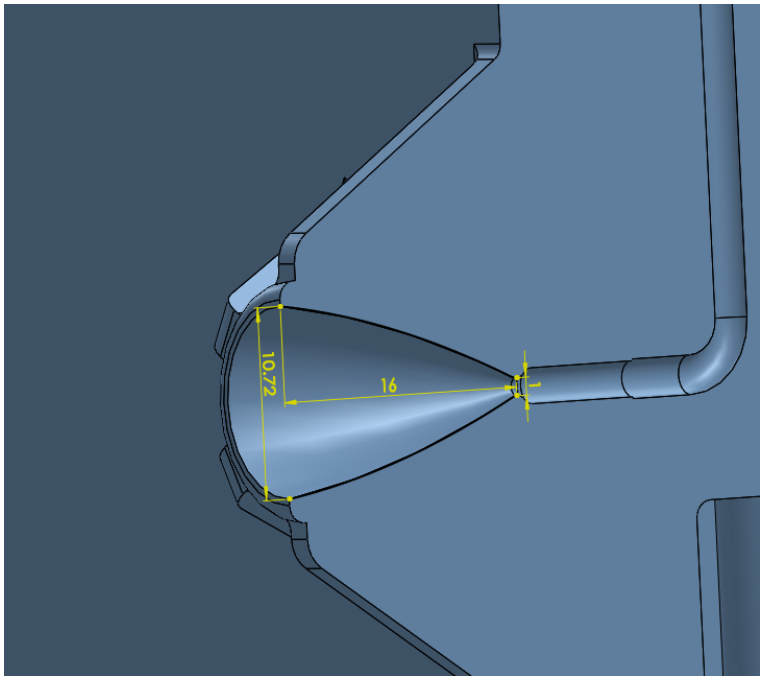

Figure 3.6: Cutaway view of the Prox-1 thruster nozzle, showing the feed pipe, throat, diverging section, and four of the six nozzle supports. Dimensions are in millimeters, showing the exit diameter, throat diameter and nozzle length.

A cutaway of the Prox-1 nozzle is shown in Figure 3.6, note the converging and diverging sections, as well as the piping feeding the nozzle.

3.5 Component Selection

This section discusses specific design decisions made during the design process. First, the propellant and printed material selections are discussed. Then, the choice of specific sensors and valves is described.

3.5.1 Propellant

The propellant chosen was R-236fa, a commercially available refrigerant marketed as a fire extinguisher. R-236fa was chosen for the Bevo 2 and INSPIRE thrusters, and it was this heritage that led to its selection by the Prox-1 team. As part of the Bevo-2 mission, the thruster containing R-236fa was approved for transport to the International Space Station, which represents a high level of safety assurance. Prox-1 will not be deployed from the station, but the additional safety verification conducted as part of this process was considered necessary for the mission. R-236fa is non-toxic and inert. The only known hazard is the risk of frostbite from direct skin contact [15]. The inherent safety of the propellant was the primary factor in its selection, since the thruster must be filled and tested in the TSL by students in a lab that lacks the facilities to handle more dangerous substances. The propellant also has a relatively high density of 1270 kg/m^3 at 50°C [13], which increases the mass that can be stored in a given volume. R-236fa has a saturation pressure of 584.2 kPa (84.5 psi) at 50°C, the maximum intended operating temperature of the thruster. With the structural safety factor of 2.5, the thruster walls must be sized to withstand an internal pressure of 1.46 MPa, a figure that is well within the capability of a 3D printed structure.

3.5.2 Printed Material

The material chosen for this thruster is a nanocomposite marketed under the name Accura Bluestone. This material is well suited for cold gas thruster applications, and has been used by the Texas Spacecraft Laboratory on the Bevo 2 and INSPIRE thrusters. Testing done by the TSL has shown Bluestone to be chemi-

cally compatible with the R-236fa propellant, and it does not outgas or degrade in vacuum. While many other suitable materials exist in the 3D printing industry, the reliability and heritage of Bluestone ultimately led to its selection.

All five metal manifolds were made from 316 stainless steel. Aluminum was considered for its lower density, but it is also weaker than steel. The manifolds have threading for different components, and the lower strength and wear resistance of aluminum threads makes them more prone to leaks, even with O-ring seals. Steel also deforms less under pressure than aluminum, which improves the quality of the O-ring seals. Future thruster designs may experiment with aluminum for mass reduction, using thicker manifold plates to mitigate the increased deformation. The only metal parts on the thruster that were not made from stainless steel were the thermal probes, which were made from copper for greater thermal conductivity.

3.5.3 Sensors

In order to obtain full knowledge of the state of the propellant in the two tanks, sensors were mounted into the tanks on metal manifolds. A pressure and temperature sensor was needed for each tank. In the plenum, the propellant will be held only as a vapor, so the pressure and temperature must both be known to determine the amount of propellant in the tank. This state can be used to estimate the thrust that the system will produce when fired, which is needed to determine how long the thruster should be fired.

In the main tank, the propellant will be stored as a saturated mixture. In principle, if either the temperature or pressure of a saturated mixture is known, the other can be determined. Despite this, the main tank was designed with both a pressure

and temperature sensor. If the telemetry is not consistent with a saturated mixture of the propellant, the most likely cause is a sensor failure. If the pressure is higher than expected for a given temperature, that indicates that the tank is completely full of liquid. The tanks have been explicitly designed to prevent this situation, which would rapidly lead to failure. A pressure lower than expected for a given temperature indicates that the tank is entirely full of vapor. This would occur if nearly all of the propellant had leaked out of the system, in which case the pressure should quickly drop to zero as the remaining vapor leaks as well. It will also occur at the end of the thruster's operational life, when nearly all of the propellant has been expelled. The satellite operations team will be able to determine if the satellite is either of these cases, and if not, a sensor error is indicated. The readings from these sensors can be used to assess the reliability of the more important sensors in the plenum.

The pressure sensor selected was an Omega Engineering PX600 subminiature pressure transducer. This sensor is capable of measuring pressures between 0 and 1.38 MPa, which encompasses the entire expected range of thruster operation, and has a burst pressure of 5.52 MPa[16], which satisfies the requirement for components to have safety factors of at least 2.5.

The temperature sensor is a simple $10k\Omega$ thermistor embedded in a copper probe with a thermally conductive epoxy. Initially, a 10 watt cartridge heater was also embedded in a copper probe and inserted into the plenum sensor plate. This heater was descoped from the mission shortly after the engineering unit was assembled, due to its high power consumption and doubtful utility. Testing of the heater showed that it required more than ten minutes to heat the plenum vapor by 2°C.

Figure 3.7: CAD model of a miniature solenoid valve from The Lee Co.

This is longer than the spacecraft could supply that level of power to the heater, and would only have a small impact on the thruster performance.The heater itself remained in place, but is no longer intended to be operated.

3.5.4 Valves

The Prox-1 thruster uses extended performance miniature solenoid valves from The Lee Company. These valves are ideal for small cold gas thruster applications, and have no analogous competitors. The valves are rated to be actuated as quickly as 500 Hz [17], but tests conducted in the Texas Spacecraft Lab have shown them to be capable of actuating as fast as 2700 Hz, if given 12 volts.

The valves are capable of withstanding pressures up to 5.5 MPa, well in excess of the pressures experienced in the Prox-1 thruster. The primary reason for their selection is their small form factor: each valve is only 6.2 mm in diameter, and has a mass of approximately 5 grams. The valves can be sealed with metal-to-metal tube fittings, which are then threaded into steel manifolds on the thruster.

Each valve is also attached to a 5 micron filter, to prevent any small particles from becoming lodged in the valve.

The valves only require the full 12 volts for a very short time. This high voltage gives the magnetic field enough strength to quickly open the armature against the high pressure gas in front of it. However, the coil inside the valve is delicate and cannot dissipate that much energy for more than a few seconds without melting and destroying the valve. The valve is capable of fully opening in less than 1 millisecond. After this time, the coil only needs to hold the armature in the open position, and the power requirements drop substantially. The voltage can be reduced to 1.8 volts, a power level that the valve can sustain without damage indefinitely. In this design, any pulse longer than three milliseconds receives 12 volts for the first three milliseconds, then only receives 1.8 volts for the remainder of the duration. Pulses shorter than three milliseconds receive 12 volts for the entire duration. This is explained in greater detail in Section 3.7.

3.6 Filling System

The Prox-1 thruster filling system is designed to fill the thruster quickly and completely while minimizing the amount of propellant spilled. The thruster has two quick disconnect filling ports attached to the main tank. External quick disconnect valves can be easily connected to and disconnected from the filling ports. These ports are double ended shutoff, meaning both sides have valves that are closed when disconnected. The valves are designed as "dry break" valves that minimize the dead volume in between the two valves, which reduces the amount of propellant that is

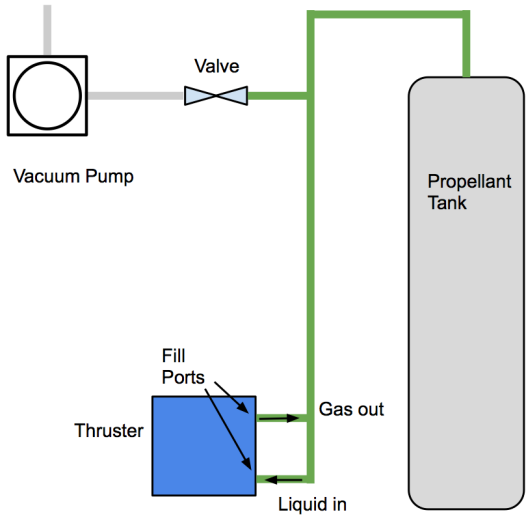

Figure 3.8: Prox-1 thruster filling system. The green lines denote tubes that carry propellant from the tank to the thruster, the gray lines indicate tubes that only hold air. The lower filling port is used to load liquid into tank while the upper port allows vapor to leave.

spilled during the fill process. A system of tubes is used to connect the propellant storage tank, the thruster itself, and a vacuum pump. This setup is shown in Figure 3.8.

Before filling the thruster, the valve to the vacuum pump is opened, and the thruster and all of the tubes are evacuated. This ensures that the thruster will only have propellant in it once the filling process is complete, not air. After the thruster has reached a low vacuum, the vacuum valve is closed, and the tank valve is opened. The propellant flows into the thruster through the lower valve. Two filling ports are used to decrease the time needed to fill the system. As the liquid propellant flows into the thruster, vapor must flow out, and a single valve would create a blockage. In this system, the higher valve allows vapor to flow out while

liquid flows in through the bottom valve. The tubes have a large internal diameter (9.5 mm), so the main lines do not prevent bidirectional flow of liquid and vapor. A second line that exhausts vapor to a lower pressure (such as atmospheric pressure) was considered in order to provide a large pressure gradient and speed the filling process, but ultimately rejected. The filling process is reasonably fast (complete filling is typically achieved within 2-3 minutes), and the vented propellant would not be recoverable without a large, complex system to capture and reliquify it.

3.7 Software and Electronics Design

Unlike previous TSL cold gas thrusters, the Prox-1 thruster was designed to have the capability to do limited onboard processing. The thruster's electronics board is equipped with an LPC1549 microcontroller, using an ARM Cortex-M3 processor [18]. The LPC1549 does not run an operating system, and is less capable than a full flight computer, but provides enough processing capabilities to run the thruster. The microcontroller has low idle power usage: the entire thruster electronics board consumes an average of 80 milliwatts when the valves are not firing.

3.7.1 Circuit Board

The electronics board contains the LPC1549 and all of its supporting electronics, including a high-precision clock reference and level shifters for the serial port connection. The board also holds voltage converters for the system. The Prox-1 spacecraft supplies the thruster with two voltage levels: 12 volts and 5 volts. The electronics board converts the 5 volt line down to 3.3 volts for the LPC1549, and 1.8 volts for the valves.

The circuit board is soldered directly to the leads of the two valves. Each valve is connected to two switches, one that supplies 12 volts, and another that supplies 1.8 volts. To operate the valves, the 12 volt switch is opened for three milliseconds to provide the high power needed to open the valve. Once open, the valve's power requirement drops significantly, as discussed previously. The circuit then switches to provide only 1.8 volts. A single valve consumes approximately 13.6 watts for the short period of high voltage, but once the voltage is lowered, the valve only consumes 300 milliwatts[17].

3.7.2 Software

The software is designed to make use of the microcontroller's hardware interrupts. Unlike software timing statements, when a hardware interrupt is triggered, the processor immediately jumps to a certain location in memory, suspending the previous action, and executes the instructions found there. The LPC1549 has several timers available that can trigger hardware interrupts. These interrupts are used to control functions that require precise timing, such as valve switching. Other, less time-critical functions, specifically message response and sensor polling, are executed in the program's "main loop", which can be interrupted.

When idle, the thruster software alternates between a sensor poll function and a message process function. The sensor poll checks all four sensors, converts the voltage levels to telemetry values, then saves the data. The message process function reads the input buffer to determine if a full message has been received. The function also generates responses to telemetry requests. The thruster is capable of accepting a variety of commands from the flight computer. The flight com-

puter can query any of the four sensors individually, or all simultaneously, and the thruster will respond with the most recent measurement(s). The thruster can also be commanded to open or close individual valves, for testing purposes. Finally, the thruster can accept a timed fire command, this is the nominal mode of operation. The thruster is given a time in milliseconds, and opens the firing valve for the specified duration.

If a fire command is received, the nozzle high voltage switch is powered, and a timer is started, running for the duration of the pulse. When this timer expires, the current operation is suspended, and the processor closes the nozzle valve. While this timer is running, the sensor poll and message process functions are still alternating. During a timed fire, if the sensor poll function detects that the plenum pressure is less than 90% of the main tank pressure, the refill valve is opened, to be closed either when the pressure recovers to 95% of the main tank or the firing sequence is complete.

Because the firing command depends on correct readings from both pressure sensors, a contingency was developed in case either sensor becomes inoperable or begins producing false values. The flight computer can send manual commands to the valves to open the nozzle for a certain time. This eliminates the advantage of onboard timing, however, and is only to be done in case of sensor failure.

When either valve is initially opened, a three millisecond timer is started. When this timer expires, an interrupt is called that turns on the low voltage line and turns off the high voltage line. This timer is halted and reset if the high voltage line closes before it expires, so pulses shorter than three milliseconds never switch to

SOH character (1 byte)
SOT character (1 byte)
Subsystem ID (2 bytes)
Command Code (2 bytes)
Parameter (plain text number, variable length)
Comma (1 byte)
(further comma-separated parameters, as needed)
Newline character (1 byte)

Table 3.1: Prox-1 data interface message format.

low voltage. These three timers (timed fire, nozzle valve voltage, and refill valve voltage) are all capable of running simultaneously without any problems.

3.7.3 Interface

The thruster was designed to use the same data interface as the other subsystems of the Prox-1 thruster. In order to ease development of systems using potentially different architectures, the Prox-1 data interface uses strings to transmit data. The message format is shown in Table 3.1.

Each subsystem on the spacecraft has a unique ID and a set of command codes, each one corresponding to one of the possible commands. The subsystem uses that command code in the telemetry response. For example, a timed fire command would be sent with the hexadecimal code 0x20, as well as a plain text parameter indicating the firing duration in milliseconds. The response would use the same command code and have no parameters, and would simply serve to indicate that the thruster received the command. A request for sensor data would have no parameters, and the response would have four plain text decimal values, separated by commas, containing the most recent data from the four sensors.

3.7.4 Timing

One of the reasons for selecting a microcontroller for onboard timing was the ability to perform more precise pulses than were previously possible. The precision of this timing was tested: a 2 ms commanded pulse resulted in a pulse with an actual duration (as measured by an oscilloscope) of an average of 2.002 milliseconds, with a standard deviation of 4 microseconds over 50 trials. This compares favorably to testing conducted on previous thrusters relying on flight computer commands, in which a 2 ms commanded pulse ranged between 2 and 6 milliseconds of actual duration.

3.8 Expected Performance

The most important performance parameters of the thruster are the thrust and specific impulse. Thrust is simply the total force that the thruster is capable of exerting. Specific impulse (abbreviated I_{sp}) is a measure of the propulsive efficiency of the system. The specific impulse is the exhaust velocity divided by the acceleration due to gravity, this is done to change the exhaust velocity into units of seconds, which are common to both SI and English measurement systems. The ΔV that the system can achieve is directly proportional to the specific impulse, as seen in Equation 3.1, so it is desired to be a high as possible. Cold gas system typically have I_{sp} values in the range of 30-70 seconds [6].

3.8.1 Thrust

The isentropic thrust equation for a nozzle [14] is:

$$F = \dot{m}V_e + P_e A_e \tag{3.2}$$

In Equation 3.2, F is the total thrust produced, $\dot{m}$ is the mass flow rate of exhaust, V_e is the exhaust velocity (equal to gI_{sp}), P_e is the pressure at the exit plane, and A_e is the area of the nozzle exit. The first term in this equation is called the momentum term, since it arises from the momentum of the exhaust gas. The second term is called the pressure term, since it arises from the pressure of the exhaust gas on the nozzle exit plane.

The mass flow rate is constant throughout the nozzle by conservation of mass, so it can be calculated most simply at the nozzle throat, where the Mach number is 1:

$$\dot{m} = \rho^* V^* A^* \tag{3.3}$$

Here, ρ^* is the density of the exhaust at the nozzle throat, V^* is the velocity at the nozzle throat (equal to the speed of sound at the throat), and A^* is the area of the nozzle throat. In a cold gas thruster, the exhaust is not at an extremely high temperature or pressure, so the ideal gas equations can be used as a reasonable approximation. This allows an expression for the density at the throat:

$$\rho^* = \frac{P^*}{RT^*} \tag{3.4}$$

Here, P^* is the pressure at the throat, R is the gas constant for the propellant, and T^* is the temperature at the nozzle throat. The speed of sound can be calculated

simply with:

$$a^* = \sqrt{\gamma R T^*} \tag{3.5}$$

Here, a^* is the speed of sound at the throat, γ is the ratio of specific heats for the exhaust (the ratio C_p/C_v is a property of the propellant, and is published in [15]), and T^* is the temperature at the throat, as above. Finally, using isentropic flow equations from [14], the pressure and temperature at the throat can be related to the conditions in the plenum.

$$P = P_t \left(1 + M\frac{\gamma - 1}{2}\right)^{\frac{-\gamma}{\gamma-1}} \tag{3.6}$$

$$T = T_t \left(1 + M\frac{\gamma - 1}{2}\right)^{-1} \tag{3.7}$$

In these equations, P_t and T_t are the pressure and temperature in the plenum (also called the stagnation conditions). These equations can be used to determine the pressure and temperature at the throat as well as the nozzle exit. At the throat, the value of M is simply 1, since the flow is sonic at the throat. At the nozzle exit, $M = M_e$, which is a function only of the nozzle geometry. To calculate the exit velocity:

$$V_e = M_e \sqrt{\gamma R T_e} \tag{3.8}$$

Finally, these equations can be brought together with Equation 3.2 to yield:

$$F = \rho^* V^* A^* M_e \sqrt{\gamma R T_e} + P_t \left(1 + M_e \frac{\gamma - 1}{2}\right)^{\frac{-\gamma}{\gamma - 1}} A_e \tag{3.9}$$

$$F = \frac{P_t \left(1 + \frac{\gamma-1}{2}\right)^{\frac{-\gamma}{\gamma-1}} \gamma A^* \left(1 + \frac{\gamma-1}{2}\right)}{\sqrt{\left(1 + \frac{\gamma-1}{2}\right)\left(1 + M_e \frac{\gamma-1}{2}\right)}} + P_t \left(1 + M_e \frac{\gamma - 1}{2}\right)^{\frac{-\gamma}{\gamma-1}} A_e \tag{3.10}$$

In practice, Equation 3.10 is unwieldy, and the preceding equations would be calculated separately, as the intermediate values are also useful. However, it is instructive to see that in the final form, the only terms present in the thrust equation are γ, a property of the propellant; A^* and A_e, simple nozzle geometry; M_e, a function of γ and nozzle geometry, and P_t, the pressure in the plenum. Other than plenum pressure, these terms are all fixed by the propellant choice and nozzle design, so the pressure can only be varied in-flight by changing the pressure of the plenum. Using a pressure of 200 kPa in the plenum, and a nozzle throat diameter of 1 mm, the thruster is expected to produce 75 mN.

3.8.2 Specific Impulse

The specific impulse is somewhat simpler to calculate than the thrust. Equation 3.8, used in the previous section, is reproduced here:

$$V_e = M_e \sqrt{\gamma R T_e} \tag{3.11}$$

The specific impulse itself is:

$$I_{sp} = \frac{V_e}{g} \tag{3.12}$$

where g is the acceleration due to gravity (9.81 m/s^2).

The specific impulse, as calculated above, only takes into account the effect of the momentum term of the thrust equation. This does not entirely capture the ability of the thruster to change the velocity of its spacecraft. To capture the pressure term as well, a property called the effective specific impulse is often used [12].

$$I_{sp,ef} = \frac{T}{\dot{m}g} \tag{3.13}$$

In Equation 3.13, T is the total thrust of the system, $\dot{m}$ is the mass flow rate, and g is the acceleration due to gravity. Note that Equation 3.13 becomes Equation 3.12 if the pressure term of the thrust is zero.

While M_e can be increased without limit by raising the area ratio of the nozzle, this is impractical. The increased expansion decreases the temperature (it can be seen from Equation 3.7 that temperature is inversely related to Mach number), which decreases the speed of sound. This limits the increase in velocity that further expansion can provide. This means that, after a certain point, the nozzle size must increase greatly to provide even a small increase in specific impulse. After several design iterations, the area ratio of 100:1 was chosen, which provides an exit Mach number of 4.022, and an effective exhaust velocity of 570.2 m/s, which gives an effective I_{sp} of 58.1 seconds.

Chapter 4

Test Environment

The EDU and flight thrusters will both be tested by the Prox-1 team at Georgia Tech, but prior to delivery the EDU was tested in the TSL's own facilities to ensure that it performed acceptably. The flight thruster will be put through similar testing. These tests will determine that the thruster does not leak, and will experimentally determine thrust and specific impulse.

4.1 Approach

The Prox-1 thruster is designed to produce very small levels of thrust, on the order of 50 mN. A continuous thrust at this small level was not measurable with the facilities available to the TSL, so the thrust was measured in very short pulses with a ballistic pendulum. These short pulses will give an indication of the thruster's performance, although it will be incomplete without a continuous thrust measurement.

4.2 Test Stand

The Prox-1 thruster's impulse was measured using a ballistic pendulum. This pendulum was suspended in front of the thruster nozzle, and when the thruster fired, it imparted an impulse to the pendulum, which swung away from the nozzle.

An encoder attached to the fulcrum of the pendulum measured the total angle of the swing. The impulse of the firing can be determined from this angle. Three assumptions were made. The first assumption is that all of the thrust is applied in an instantaneous impulse. The second assumption is that all of the thrust is captured by the pendulum's pusher plate. Both of these assumptions work well when the thrust applied is very small and over a very short time period. As the thrust duration increases, both assumptions become less valid. The instantaneous impulse assumption is clearly less valid for longer pulses, and as the pendulum swings away from the nozzle exit plane, it intercepts a smaller share of the exhaust gas, and captures less of the thrust. The third assumption is that the pendulum bearings are frictionless. This assumption is most valid when the swing rate of the pendulum is low, and higher-order frictional terms become negligible. The test stand geometry is shown in Figure 4.1.

The design of the test stand was driven by two considerations. The first consideration was maximizing the deflection angle of the pendulum for small impulses. This reduces the impact of the quantized steps of the encoder on the uncertainty in the thrust measurements. The second consideration was minimizing the angular velocity of the pendulum, to reduce the effect of friction in the bearings. Both of these considerations can be met by making a relatively heavy, well balanced pendulum with a long moment arm. The high moment of inertia reduces the angular velocity of the pendulum for a given momentum, satisfying the second condition. The large ratio of the thruster moment arm to the center of mass moment arm increases the swing angle by reducing the restoring torque of gravity relative to the initial angular momentum.

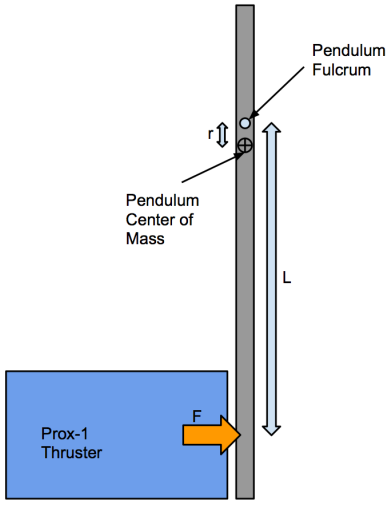

Figure 4.1: Ballistic pendulum test stand geometry, showing the force F from the thruster, the thrust moment arm L, and the center of mass moment arm r.

4.3 Thrust Calculation

The potential energy of the pendulum with respect to its "rest" state can be calculated from the maximum height that the center of mass of the pendulum reaches:

$$E = mg\Delta h \tag{4.1}$$

$$E = mgr(1-cos\theta) \tag{4.2}$$

In Equation 4.2, E is the potential energy of the pendulum, m is the mass of the pendulum, g is the acceleration due to gravity, r is the distance from the center of mass of the pendulum to its fulcrum, and θ is the maximum swing angle of the pendulum. Using the assumption that this energy was imparted instantaneously, and

the assumption that no energy is lost to friction, this energy can be equated to the kinetic energy of the pendulum immediately after the impulse. The kinetic energy of a rotating object is:

$$E = \frac{1}{2} I \omega^2 \tag{4.3}$$

$$\omega = \sqrt{\frac{2E}{I}} \tag{4.4}$$

Here, E is the energy of the object, I is the moment of inertia about the axis of rotation, and ω is the angular velocity. The angular impulse applied to the object is:

$$\Delta L = \omega I \tag{4.5}$$

In Equation 4.5, ΔL is the angular impulse, ω is the angular velocity, and I is the moment of inertia. Finally, the linear impulse imparted to the pendulum can be found using the moment arm d and the impulse J:

$$J = \frac{\Delta L}{d} \tag{4.6}$$

These equations can be brought together to produce an expression for the linear impulse imparted if the deflection, geometry, and mass properties of the pendulum are known:

$$J = \frac{\sqrt{2mIgr(1 - cos(\theta))}}{d} \tag{4.7}$$

To determine the average thrust of a pulse of finite (but small) time, the linear impulse is divided by the pulse time, so the equation for average thrust is:

$$T_{avg} = \frac{\sqrt{2mIgr(1-cos(\theta))}}{d\Delta t} \tag{4.8}$$

The mass of the pendulum is 0.012 ± 0.0005 kg, the moment of inertia is $2.304 \times 10^{-4} \pm 10^{-6}\ kg - m^2$, the fulcrum to center of mass distance is 0.034 ± 0.001 m, and the length of the pendulum is 0.247 ± 0.001 m. The uncertainty in the pulse length was taken from the approximate timing error determined from the microcontroller, $\pm 3 \times 10^{-6}$ s. The uncertainty in the deflection of the pendulum was taken to be half of the encoder step size. This step size can be found by dividing 2π radians by 2^{10}, since the encoder has a 10 bit ADC. The step size is 6.14×10^{-3} radians, so the uncertainty is $\pm 3.07 \times 10^{-3}$ radians.

During the tests conducted, the uncertainty was largely due to the discretized steps of the encoder. This produces large uncertainties, on the order of ± 16 mN for very short pulses of 2 milliseconds. Longer pulses produce more total impulse, which leads to a larger angle. This reduces the effect of the discretization by making the uncertainty a smaller fraction of the overall value. Because of this, longer pulses have lower uncertainties. The 10 millisecond pulses tested only had an uncertainty level of ± 2.4 mN.

4.4 Vacuum Chamber

The Texas Spacecraft Laboratory is fortunate to have a small vacuum chamber capable of reaching microtorr-level vacuum. The vacuum chamber features a

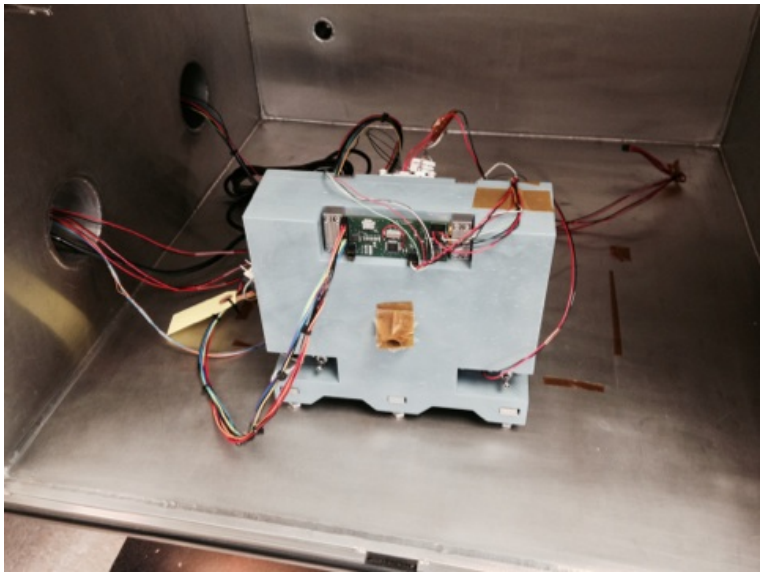

Figure 4.2: Prox-1 EDU thruster in TSL vacuum chamber.

liquid nitrogen cold trap to condense gasses in the chamber and reduce the load on the chamber pump. This is especially useful for thruster testing, since it decreases the time after each pulse that the chamber requires to return to a high vacuum. The vacuum chamber is shown in Figure 4.2 with the EDU thruster inside and the door open. The two holes on the left of the image are passthroughs for cables and the hole at the back connects to the pump. The presence of this vacuum chamber greatly simplified the testing process, since no special permission or scheduling was needed to use it. The chamber is large enough to test the thruster, but not so large that it is expensive to operate. The vacuum chamber is not equipped with thermal control, so the thruster was only tested at ambient conditions, approximately 20-25°C.

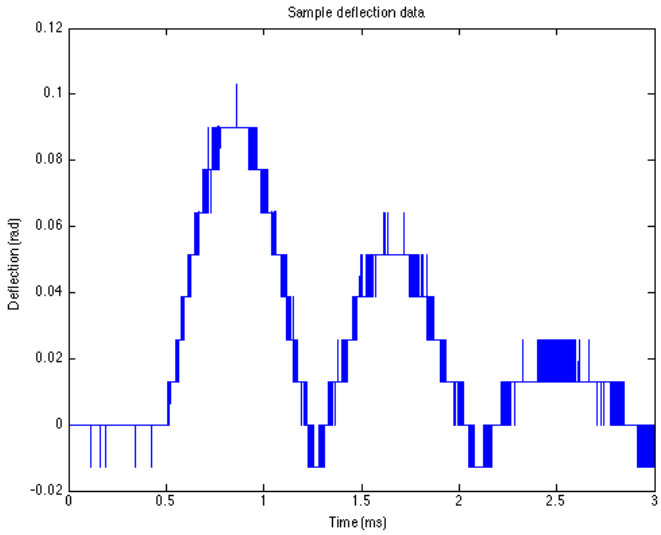

Figure 4.3: Sample deflection data from a thruster pulse, showing the initial swing and two rebounds. Note the 'stairstepping' caused by the quantized steps of the encoder.

4.5 Data Acquisition and Processing

The angular deflection of the pendulum was measured with a 10 bit US Digital miniature encoder. The encoder converts the angular position of its shaft (attached to the pendulum) to a voltage. The ADC present on the encoder has a resolution of 10 bits, so the encoder can detect 2^{10} or 1024 positions per full revolution. This leads to quantized jumps in the raw data, as seen in Figure 4.3.

In Figure 4.3, dark vertical bands of varying width can be seen between the step transitions. These bands are caused by rapid oscillation of the voltage between the 'low' and 'high' sides of the transition. Figure 4.4 shows one such step transition magnified to show this effect.

The encoder voltage was read by a National Instruments data acquisition

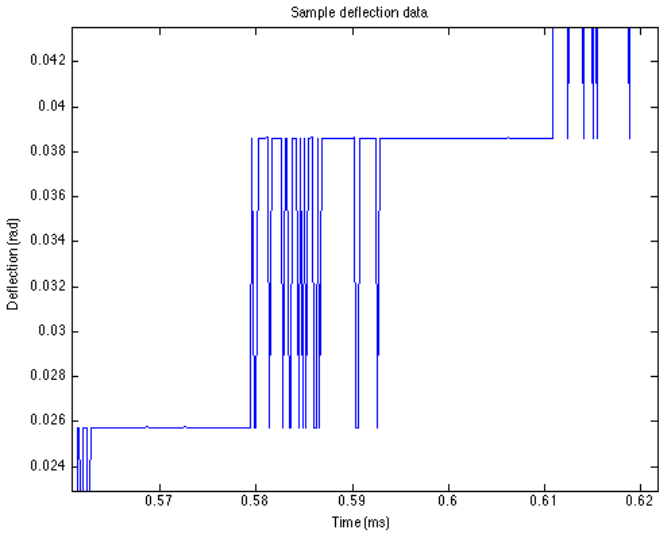

Figure 4.4: Magnified view of a step transition, showing the rapid oscillation between voltage levels.

device. A Labview VI was used to import the data from the DAQ and convert the voltage value to angular deflection. The data were then imported into Matlab, where the peak deflections of each pulse were determined. During the testing, the plenum pressure was monitored and recorded, and used to determine when the plenum needed to be recharged.

Chapter 5

Data Analysis

Prior to delivery to Georgia Tech, the EDU thruster was tested by the TSL. The purpose of the testing was twofold. First, to verify that the unit performed acceptably before delivery to the Prox-1 team. Second, to validate the testing apparatus that the TSL has used for its cold gas thrusters. Georgia Tech has a much more extensive propulsion system testing facility, which the Prox-1 team has access to. They will be carrying out more precise characterization of the thruster in those facilities in early summer 2015, prior to assembly of the flight unit. Comparing the data from the TSL testing with the Georgia Tech testing should also help to determine the accuracy of the TSL's test apparatus.

5.1 Leak Testing

The first test conducted was a leak check. Each of the twelve O-ring seals used in the thruster represents a potential leak site, and printing errors could introduce small cracks into the plastic. The thruster will have to be filled prior to delivery to the launch provider, and will likely have to remain filled for several months prior to launch. Over this relatively long time scale, even a small leak could cause a substantial loss of propellant.

The EDU was checked for leaks before any other testing commenced. The

thruster was filled with approximately 400 grams of propellant for the test. The plenum was charged to 200 kPa, which corresponds to 7.4 grams of propellant at 25°C. The thruster was massed and placed in the vacuum chamber for 192 hours. When massed after the test, the thruster was found to have the same mass, within the 1 gram tolerance of the scale. This places an upper limit on the leak rate of the thruster of 5.2 milligrams per hour. Over a one year period, this maximum rate would cause the loss of 45.7 grams of propellant assuming a constant leak rate, or 2.5% of the total propellant load. Note that this test only places an upper bound on the leak rate, since no leak could be measured with the available equipment.

It should be noted that the leak check here only demonstrates that the thruster *as assembled for the test* was relatively free of leaks. When a manifold is removed and reattached, there is some risk of an assembly error that causes an imperfect seal by one of the o-rings. Thus, the flight thruster must be given a leak check after final assembly to ensure that the thruster will not leak before or during the mission.

5.2 Thrust Testing

The EDU thruster was tested at three different plenum pressures: 200 kPa, 175 kPa, and 150 kPa. All of the tests were conducted at 25°C, due to the lack of thermal vacuum facilities. Three different pulse times were tested at each pressure: 2 ms, 5 ms, and 10 ms. Fifty pulses were conducted at each of these conditions, for a total of 450 firings. The average thrust of the pulse was calculated, as described in section 4.3. Figure 5.1 shows the average thrust of each of the pulses conducted at 200 kPa.

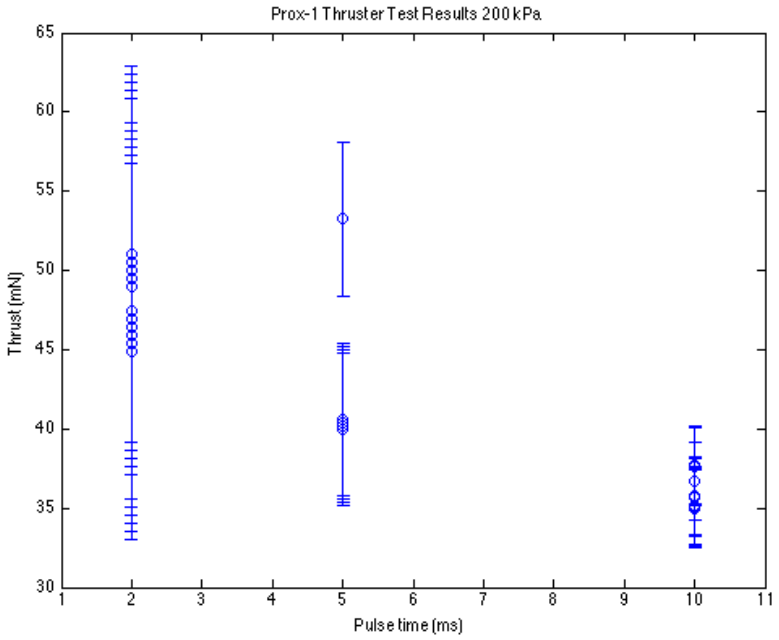

Figure 5.1: Average thrust (in mN) of each pulse conducted at 200 kPa plenum pressure.

Note that the error bars are extremely large for the short pulses. This is due to the quantized step angle of the encoder relative to the number of steps that the pendulum traverses. Very short pulses produce a small deflection angle, corresponding to only three or four steps of the encoder, producing up to a 33% uncertainty in the position.

The 2 ms pulses have a thrust level of 50 ± 16 mN, and the measured thrust decreases as the pulse time lengthens. The 5 ms pulses (with the exception of one outlier) have a thrust level of 40.2 ± 4.8 mN, and the 10 ms pulses have a thrust of 35.7 ± 2.5 mN.

It is clear from Figure 5.1 that the measured thrust decreases as the pulse time increases. This was previously believed to be caused by the motion of the pendulum away from the exit plane of the nozzle during the pulse, but new high rate measurements show that this is most likely not the case. Figure 5.2 shows the smoothed time series deflection of the ballistic pendulum. From the figure, the deflection of the pendulum is approximately 1.58 milliradians at the end of the pulse. This corresponds to a distance from the exit plane of 0.39 millimeters. This very small distance is unlikely to cause any loss of thrust. The consequences of this are discussed in section 5.5.

The average thrust for the 150 pulses made at 175 kPa and 150 kPa is shown in Figures 5.3 and 5.4, respectively.

The same loss of thrust is observed to occur at the lower pressures as well. Additionally, at the lower pressures, the overall thrust is reduced compared to higher pressures. This result is expected from the isentropic flow equations. From section

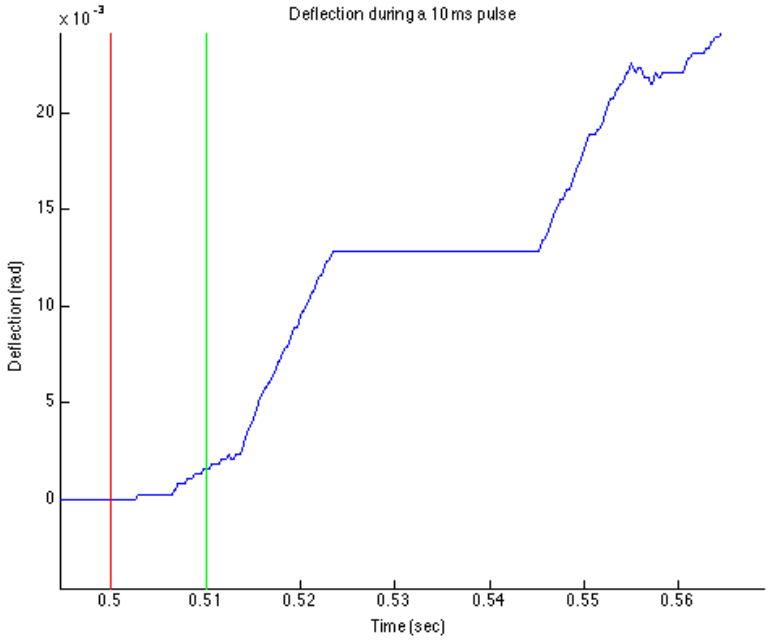

Figure 5.2: Smoothed time series of pendulum deflection during a sample 10 millisecond pulse, from valve opening (red vertical line) to valve closing (green vertical line).

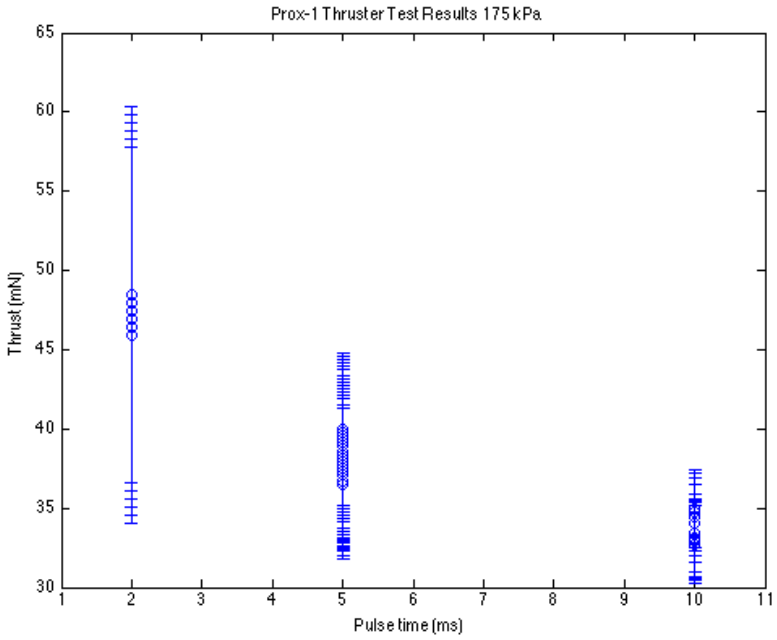

Figure 5.3: Average thrust (in mN) of each pulse conducted at 175 kPa plenum pressure.

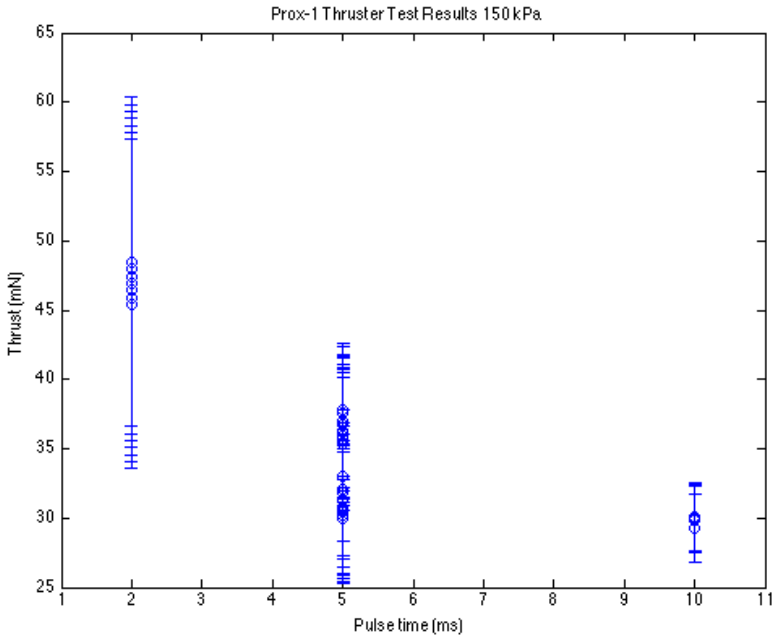

Figure 5.4: Average thrust (in mN) of each pulse conducted at 150 kPa plenum pressure.

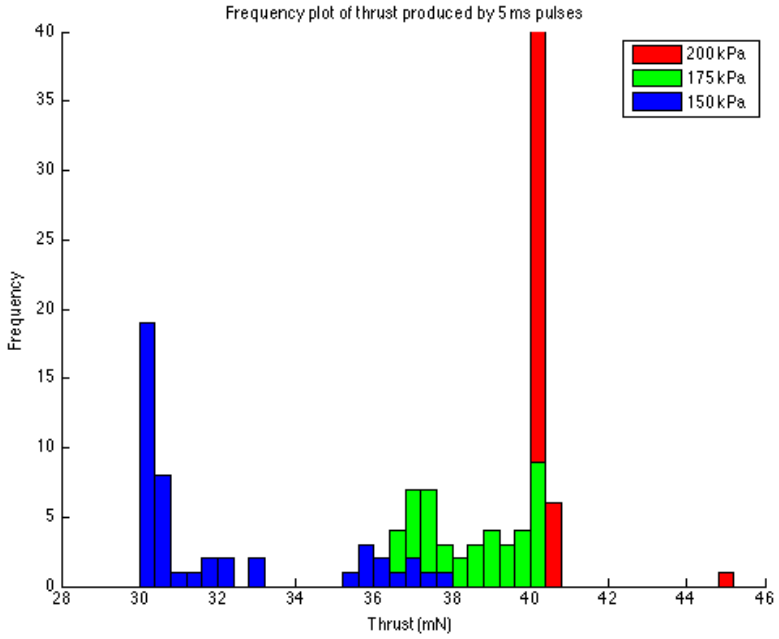

Figure 5.5: Histogram plot of thrust produced by 5 millisecond pulses at three different plenum pressures.

3.8, the thrust is expected to be proportional to the plenum pressure. The thrust of the pulses produced at each pressure appear to follow this proportionality. A histogram plot of the thrusts measured from 5 millisecond pulses is shown in Figure 5.5. The 175 kPa pulses have a slightly higher thrust than expected, nearly as high as the 200 kPa pulses. However, the pulses clearly follow the expected trend of lower thrust at lower pressure.

5.3 Specific Impulse Estimation

The effective specific impulse was discussed previously, Equation 3.13 is reproduced below:

$$I_{sp,ef} = \frac{T}{\dot{m}g} \tag{5.1}$$

The uncertainty of this equation can be calculated using standard error propagation methods:

$$\sigma^2_{I_{sp,ef}} = \left(\frac{1}{\dot{m}g}\sigma_T\right)^2 + \left(-\frac{T}{\dot{m}^2 g}\sigma_m\right)^2 \tag{5.2}$$

In Equation 5.2, $\sigma_{I_{sp,ef}}$ is the uncertainty in the effective specific impulse, σ_T is the uncertainty in the thrust, and σ_m is the uncertainty in the mass flow rate. Note that since the standard acceleration due to gravity is an exactly defined constant, it has no error term.

The thrust of the unit was determined in the previous section, so the mass flow rate must also be determined. To do this, the thruster was fired for a total of 100 seconds, in a series of 2 ms pulses (total of 50,000 pulses). Since the I_{sp} is temperature-dependent, the temperature was allowed to stabilize at 20°C before beginning the test. The thruster was massed before and after the test, and found to have experienced a total mass loss of 9.2 ± 0.05 grams. This gives a mass rate of $9.2 \times 10^{-5} \pm 5 \times 10^{-7}\ kg/s$. The thrust used in this calculation is the impulse thrust calculated in the previous section at 200 kPa: 50 ± 16 mN, since that matches the pressure and pulse duration used in the I_{sp} determination.

Using the equations above, the $I_{sp,ef}$ was determined to be 55.4 ± 17.7 seconds. This is a very large uncertainty level, ranging from unacceptably low (37.7 seconds, requiring nearly 3 kg of propellant) to unreasonably high. Nearly all of the uncertainty is due to the large uncertainty in the thrust level. Since the thrust will

be more precisely characterized at the Georgia Tech facilities, the specific impulse uncertainty can be greatly reduced.

5.4 Blowdown Test

A plenum blowdown test was also conducted on the EDU to measure the pressure loss with the nozzle held open. The plenum was first pressurized to approximately 200 kPa from the main tank. After waiting for the temperature to stabilize, the nozzle was opened and the plenum was vented into the vacuum chamber. The pressure in the plenum was monitored during the test at one sample per second. The ballistic pendulum was also placed in front of the thruster for the test. Since the ballistic pendulum is only capable of measuring fast impulses, it cannot measure the actual thrust produced during the 240 seconds of this test. It can, however, provide a qualitative measure of the thrust, since higher continuous thrust will keep the pendulum suspended at a higher angle. The results of this test are shown in Figure 5.6.

During the test, the pressure in the vacuum chamber rose to 10^{-4} torr, which still provided a large enough pressure ratio to approximate a space environment.

As expected, the pressure in the plenum drops while the nozzle is open. The ballistic pendulum oscillates at the beginning of the test, before settling into a slowly decaying deflection angle. This indicates, again, as expected, that the thrust is dropping with the pressure.

The temperature in the plenum remained relatively stable between 20°C and 25°C during the test. Using this temperature, and the ideal gas equation, the density

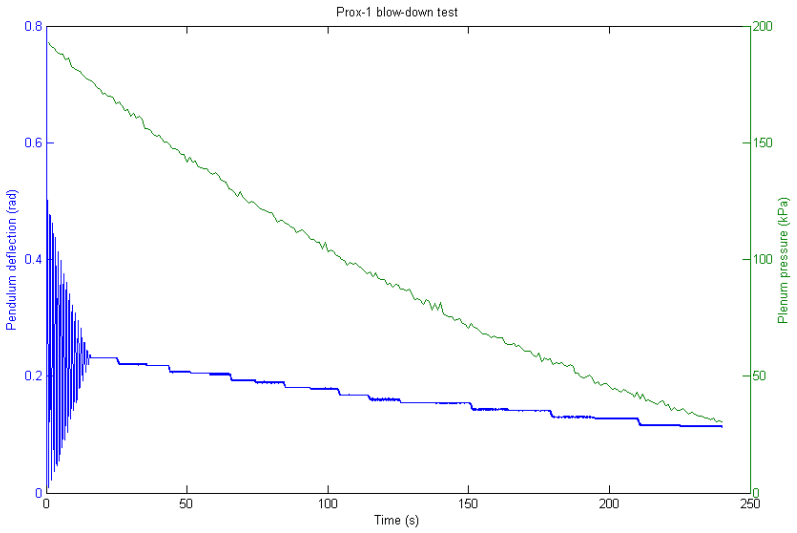

Figure 5.6: Plenum pressure and pendulum deflection during the thruster EDU blowdown testing.

of the propellant remaining in the tank can be estimated with:

$$\rho = \frac{P}{RT} \tag{5.3}$$

where ρ is the density of the gas in kg/m^3 or g/L, P is pressure in Pa, R is the gas constant for the propellant (54.68 $J/kg-K$), and T is the temperature in Kelvin. Figure 5.7 shows the density as a function of time.

Using the known volume of the plenum, the mass of the propellant inside can be calculated. This in turn allows the calculation of the mass flow rate throughout the test, shown in Figure 5.8.

The mass flow rate here, beginning at approximately 4.5×10^{-5} kg/s, is substantially lower than the mass flow rate calculated from the series of pulses

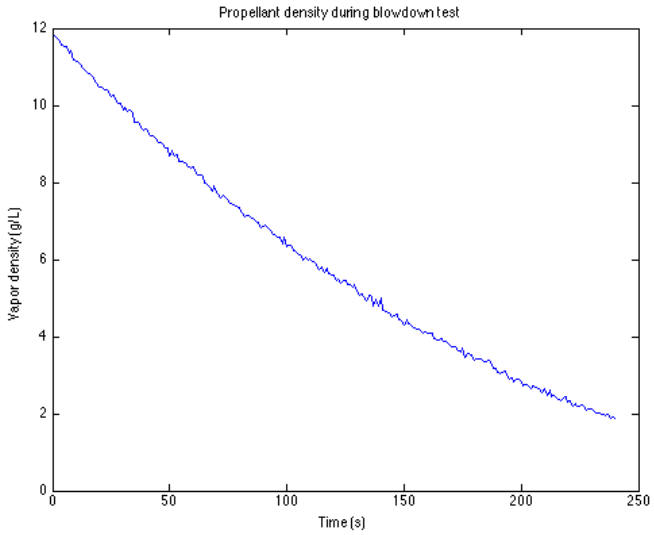

Figure 5.7: Plenum propellant density during blowdown test.

(9.2×10^{-5} kg/s). This is supported by the corresponding difference in the thrust levels between short pulses and longer ones.

5.5 Summary of Results

There were four discrepancies discovered during the testing of the thruster.

1. The thrust of the unit decreased substantially as the pulse time was increased, dropping from approximately 50 mN (2 ms pulse) to 35 mN (10 ms pulse).

2. The thrust of the unit, even from a short pulse, was lower than predicted from the isentropic flow equations (75 mN).

3. The fast-pulse mass flow rate (9.2×10^{-5} kg/s) measured from a series of 2 ms pulses was lower than the predicted mass flow rate.

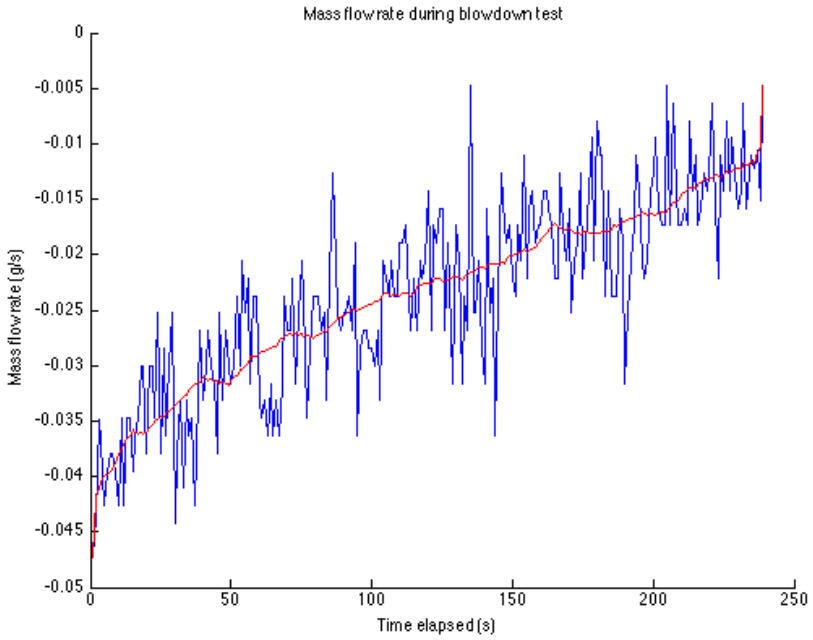

Figure 5.8: Mass flow rate out of the plenum during the blowdown test (blue) and time-averaged mass flow rate (red). Note that the negative sign simply means the mass is flowing outwards.

4. The mass flow rate of the thruster in continuous mode (4.5×10^{-5} kg/s) was substantially lower than the fast-pulse mass flow rate.

The most likely explanation for the thrust being lower than the isentropic flow predictions is that the thruster is a non-isentropic system. The exhaust must travel through a pipe to the nozzle before being expelled, and this pipe introduces friction into the flow. 3D printing can introduce surface roughness that, especially on small features, can be a significant fraction of the feature size. This roughness impedes the flow, reducing thrust and mass flow rate, but not specific impulse. This is not unexpected, and explains #2 and #3. Significantly, the specific impulse measured here was similar to the expected value, though the uncertainty interval is large.

However, there was an additional loss experienced for longer pulses, in both thrust and mass rate. This indicates that, after an initial burst of high thrust, the steady-state thrust is much lower than expected. This is supported by the reduced mass flow rate, which could not support the higher levels of thrust seen in the short pulses. There are many possible explanations of this, including that the test methodology was flawed in its estimation of long-duration thrust. The higher precision data from Georgia Tech's testing of the EDU should help determine the cause. If the steady state thrust truly is lower than the thrust requirement, the nozzle size and feed pipe sizes can be increased to raise the thrust.

Table 5.1 shows a summary of various important performance metrics as measured on the EDU thruster.

Metric	Value
Dry Mass	3584 grams
Wet Mass	5422 grams
Max Operating Pressure	584 kPa
Burst Pressure (theoretical)	1.46 MPa
Thrust (short pulse)	50 ± 16 mN
Thrust (long pulse)	35 ± 2.4 mN
Specific Impulse	55.4 ± 17.7 s
Prox-1 ΔV (theoretical)	15.7 m/s
Power Consumption (idle)	80 mW
Power Consumption (firing)	380 mW
Power Consumption (pulse)	13.7 mW

Table 5.1: Prox-1 EDU thruster performance metrics. All values not indicated as theoretical were experimentally determined.

Chapter 6

Further Research

During the development and testing of the Prox-1 thruster, several areas were noted that could be improved upon in future systems.

6.1 Test Stand Improvements

One of the largest problems with the thruster characterization was the large uncertainty in the measurement of the thrust. This was primarily due to the coarse resolution of the encoder used. The test apparatus had a 10 bit ADC, which permitted measurements in steps of approximately 0.35°. When very small impulses were applied, the total deflection of the pendulum was as small as 1 degree, or 3 steps of the encoder. This led to a very large uncertainty in the position of the pendulum relative to the deflection, which in turn produced a large uncertainty in the thrust.

To decrease this uncertainty, either a more precise encoder can be used, or the pendulum can be made to swing farther. More precise encoders are available, but are more expensive and generally larger than the one used in this apparatus. Balancing the pendulum to bring the center of mass closer to the fulcrum would make the pendulum swing farther, given the same impulse. Other methods of measuring thrust than a ballistic pendulum could also be considered. A sensitive load cell could detect the small thrust levels produced by the thrusters such as this one,

and would be capable of measuring longer firings.

Another critical measurement is the steady state thrust of the unit. The large differences discovered between the short and long pulses indicates that any future thrusters intended for continuous mode operation (as opposed to pulsed mode) will require more extensive characterization with a test apparatus designed to measure longer pulses.

6.2 New Printing Materials

The Bluestone material used in this thruster has been very reliable and is a good material for cold gas propulsion systems. However, the 3D printing industry has advanced rapidly, and many other candidate materials are available for future projects.

New advancements in additive manufacturing of metal components raises the possibility of producing cold gas thrusters similar to the one described here out of metal. The thruster structure would still be made with additive manufacturing, which would allow the complex internal geometries described here. Additionally, a metal thruster could be machined after the printing process to add features such as threads. This would eliminate the metal manifolds required for sensors, fill ports, and valve fittings. This would not only reduce the complexity and cost of the unit, but it would allow the volume currently occupied by support material for the manifolds to be used for propellant storage.

Additionally, a thruster printed from aluminum or steel would have higher resistance to internal pressure, due to the superior tensile strength of these metals

compared to printed plastics. This could be used to thin the tank walls and increase the volume available to the propellant, or to store the propellant under higher pressure. This would allow the use of different propellants that could potentially provide higher thrust.

Unfortunately, metal printing also introduces problems. Metal printed parts typically have higher surface roughness than equivalent plastic printed parts. This could exacerbate the issues encountered here with loss of thrust. Metal parts are also printed with metal supports, which are more difficult to remove from interior features like tanks and pipes. This could result in blockages in the propellant lines or loss of tank volume to internal supports. These problems will have to be explored and more completely understood before printed metal thrusters can be used.

6.3 Radiation Hardening

One area in which small satellites are become more feasible is interplanetary missions. Thrusters such as this one will be necessary for such missions, for both attitude control and trajectory correction. Such missions will be exposed to higher levels of radiation than Earth-orbiting satellites, and they will be required to operate for many years in transit to their destinations. All components for such a mission, including propulsion systems, will require extensive characterization in how they respond to radiation. Onboard electronics will have to be radiation hardened, and the printed material will have to be studied for any degradation in high radiation environments.

6.4 Control Changes

The Prox-1 thruster relies on commands from the flight computer to determine the duration of the pulses. While the thruster will faithfully execute a pulse of the commanded duration, it has no ability to determine how much momentum was actually imparted. Since the thruster electronics board has access to temperature and pressure information of the plenum, it is theoretically possible for the unit to determine how much thrust can be developed at the current state, and can fire for the correct amount of time. This would allow the flight computer to simply send a desired impulse level to the thruster, which would calculate the burn duration.

Chapter 7

Conclusion

The 3D printed cold gas thruster discussed here represents one of the areas in which small satellites are rapidly developing. The versatility and low cost of 3D printing make systems such as this well suited to small satellite missions. The control system and electronic interface of this thruster has allowed more precise control of the system than was previously possible. While the higher-precision characterization of the thruster has introduced questions about the ability of the unit to produce adequate thrust in continuous operation, it also represents an improvement over previous testing of such systems. Propulsion systems such as this one will continue to grow in capability, and will help small satellites further expand their role in future space missions.

Bibliography

[1] M. Meyer, L. Johnson, B. Palaszewski, D. Goebel, H. White, and D. Coote, "In-Space Propulsion Systems Roadmap," NASA, April 2012.

[2] "Welcome to Your Planet." [Online]. Available: https://www.planet.com/

[3] "NASA - GeneSat-1," 3 2007. [Online]. Available: http://www.nasa.gov/centers/ames/missions/2007/genesat1.html

[4] "ESTCube," 2013. [Online]. Available: http://www.estcube.eu/en/home

[5] K. Brumbaugh, H. C. Kjellberg, E. G. Lightsey, A. Wolf, and R. Laufer, "In-Situ Sub-Millimeter Space Debris Detection Using CubeSats," in *35th AAS Guidance & Control Conference*, Breckenridge, CO., February 2012.

[6] W. Larson and J. Wertz, *Space Mission Analysis and Design*. Microcosm, 1999.

[7] D. Hinkley, "A Novel Cold Gas Propulsion System for Nanosatellites and Picosatellites," vol. 22. Logan, Utah: AIAA/USU Conf. Small Satellites, 2008.

[8] (2015, April) 3D Printing In Zero-G Technology Demonstration. [Online]. Available: http://www.nasa.gov/mission_pages/station/research/experiments/1115.html

[9] "About the University Nanosat Program," 2013. [Online]. Available: http://prs.afrl.kirtland.af.mil/UNP/About.aspx

[10] S. Chait and D. Spencer, "Prox-1: Automated trajectory control for on-orbit inspection," in *37th AAS Guidance & Control Conference*, Breckenridge, CO., 2014.

[11] "LightSail," 2014. [Online]. Available: http://sail.planetary.org/

[12] P. Hill and C. Peterson, *Mechanics and Thermodynamics of Propulsion*, 2nd ed. Addison-Welsey Publishing Company, 1992.

[13] "Thermodynamic properties of dupont suva 236fa," DuPont, Tech. Rep., 2005.

[14] J. Anderson, *Modern Compressible Flow with Historical Perspective*. McGraw-Hill, 2003.

[15] "Hfc-236fa clean agent: Properties, uses, storage, and handling," DuPont, Tech. Rep., 1999.

[16] "Subminiature flush diaphragm pressure transducer," Omega Engineering, Tech. Rep., 2014.

[17] "Extended performance solenoid valves," The Lee Company, Data Sheet, 2014.

[18] "Lpc15xx data sheet," NXP Semiconductors, Tech. Rep., 2014.